

A MULTISCALE ANALYSIS OF HYGROEXPANSION IN WOOD

Sara Florisson¹, Marie Hartwig-Nair², Nil Tabudlong Jonasson³, Klara Hackenstrass⁴, Erik Kristofer Gamstedt⁵, Malin Wohlerl⁶

ABSTRACT: Hygroexpansion of wood is a complex phenomenon influenced by structural characteristics of wood at different length scales. A multiscale research strategy is presented that combines atomistic and continuum modelling to cross the nano into higher scales. The strategy also uses non-destructive X-ray techniques, such as small- and wide-angle X-ray scattering and X-ray computed tomography to incorporate the variability of material and validate the aforementioned numerical models. Three case studies are discussed that combine atomistic and continuum modelling to do property prediction for continuum modelling and behavioural prediction of phenomena associated with hygroexpansion, such as moisture diffusion in nano pores, symmetry class and size dependency of the elastic tensor of cellulose, and the effect of lignin on the swelling behaviour of branch wood. The results show how complex information transfer can be between atomistic and continuum modelling, but also how the inclusion of nanoscale observations into microscale predictions can lead to better insights into the hygroexpansion of wood.

KEYWORDS: hygroexpansion, multiscale, small and wide-angle X-ray scattering, X-ray full field tomography, molecular dynamics, finite element modelling

1 – INTRODUCTION

1.1 HYGROEXPANSION IN WOOD

The wood cell wall is nearly non-porous when in complete dry state. By absorption of water into the cell wall, nano-pores are created and swelling is induced. Hygroexpansion, or moisture-induced shrinkage and swelling, refers to the dimensional (volume or length) changes of material caused by changes in moisture content. Swelling is related to the dry state, whereas shrinkage is related to the water-saturated state (Engelund Thybring et al., 2022), i.e. fibre saturation point (FSP).

Hygroexpansion in wood involves physical phenomena at multiple length scales that can simply be divided into the nano, micro, meso and macro scale, see **Figure 1**. At the nanoscale, water molecules move into the cell wall during absorption, where the molecules classify as hydrogen bonded, molecular solution, absorbed in holes, or water clusters (Jakes et al., 2019). Diffusion in a solid, such as wood, is complex and depends on the interrelations between

free volumes (volume not occupied by atoms, i.e. nano-pores) in the wood matrix, molecular motions of lignin, hemicellulose and cellulose, the solubility of moisture in the wood matrix, the size of water compared to the matrix, and the high swelling pressure of wood (Jakes et al., 2019).

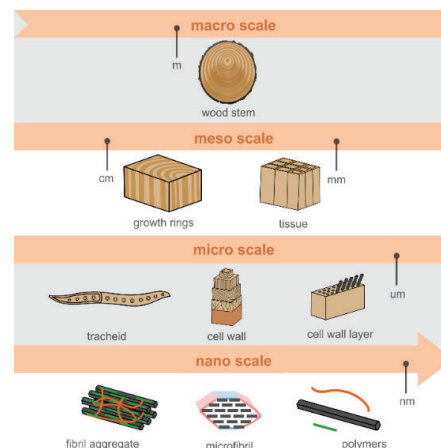


Figure 1: Categorisation of different structural features of wood into hierarchical level.

¹ Sara Florisson, Materials Science and Engineering, Uppsala University, Uppsala, Sweden, sara.florisson@angstrom.uu.se

² Marie Hartwig-Nair, Same Department, Same University, marie.hartwig@angstrom.uu.se

³ Nil Tabudlong Jonasson, Same Department, Same University, nil.tabudlong.jonasson@angstrom.uu.se

⁴ Klara Hackenstrass, Same Department, Same University, klara.hackenstrass@angstrom.uu.se

⁵ Erik Kristofer Gamstedt, Same Department, Same University, kristofer.gamstedt@angstrom.uu.se

⁶ Malin Wohlerl, Same Department, Same University, malin.wohlerl@angstrom.uu.se

The moisture content range between 0.05 g g⁻¹ and 0.30 g g⁻¹ can be referred to as the hygroscopic range (Engelund Thybring et al., 2022) and ends in the water-saturated state, after which it continues into the over-hygroscopic range. In the over-hygroscopic range, capillary water becomes increasingly more dominant, and the dimensional changes seen during hygroexpansion eventually diminish at moisture content above 0.40 and 0.45 g g⁻¹ (Engelund Thybring et al., 2022).

Fernando et al. (2023) used electron microscopy to identify cellulose, hemicellulose and lignin in the S2 layer of the wood cell wall, and therewith also visualised a nano-pore network for Norway spruce. The fundamentals behind the formation of nano-pores is not fully elucidated yet. However, it is known that water resides within the matrix rich regions (Engelund Thybring et al., 2022; Jakes et al., 2019; Pajaanen et al., 2022) and between the elementary fibrils of the cellulose aggregates due to the hydrophilic fibril surfaces (Chen et al., 2022). The latter results in an increased fibril-to-fibril distance during moisture uptake. The cellulose fibrils are not distributed uniformly (Fernando et al., 2023), but tend to aggregate irregularly between regions. The swelling of polysaccharides like cellulose is enthalpy driven and generates pressure (Jakes et al., 2019; Nishiyama, 2023). The pressure generated within the cell wall during swelling can result in deformations of microfibrils (Engelund Thybring et al., 2022).

Pajaanen et al. (2022) used a combination of X-ray scattering and molecular dynamics to study the change in microfibril bundles when swelling. At moisture content between 0 and 15 %, small water clusters formed in the cell wall matrix, which distorted the cellulose crystals. The matrix reorganised and formed nano-pores. Zhang et al. (2021) observed with molecular dynamics simulations that matrix swelling was less pronounced at lower moisture content (< 15 %) due to available voids that can collect water. At higher moisture content (15 % - FSP), the microfibril bundles start to swell and an increase in fibril-to-fibril distance is seen. Pajaanen et al. (2022) suggests that around 15% moisture content, the hemicelluloses soften and the matrix becomes more flexible and can accommodate more water. Zhang et al. (2021) and Hartwig-Nair et al. (2025) showed through atomistic modelling that hemicelluloses and lignin also contribute to the swelling of the cell wall. A volumetric increase was seen when lignin and hemicellulose interacted with water, which corresponded to a swelling coefficient of 0.343 – 0.353 and 0.198 – 0.340, respectively. Lim (2024) gave insight into the importance of lignin when it comes to wood shrinkage. Using various experimental techniques, the stability of wood showed

unaffected after delignification. However, after drying, the cellulose structure collapsed. This suggests that lignin plays a pivotal role in wood-water interaction.

The S2 layer of the cell wall is strongly reactive to water. Experiments have shown that isolated latewood S2 layer behaves highly anisotropic when ab- or desorbing moisture (Rafsanjani et al., 2014). The volumetric swelling of the S2 layer fragment is also much larger than its tissue counterpart. The microfibril angle, i.e. the angle between the cellulose microfibril and the longitudinal direction, influences hygroexpansion. Lanvermann et al. (2013) found a higher microfibril angle in earlywood, with a slow decrease towards latewood. Compression wood found in stem or branches have a much larger microfibrillar angle than normal wood, resulting in a smaller difference between longitudinal and transverse swelling (Hartwig-Nair et al., 2024; Rafsanjani et al., 2014). However, there are several suggestions that the microfibril angle is not the only explanation for swelling differences seen between longitudinal and transverse direction, or between different types of wood structures (Hartwig-Nair, 2024; Rafsanjani et al., 2014). Hartwig-Nair et al. (2024) showed a much higher longitudinal swelling for compression wood compared to opposite wood in branches, despite the microfibril angle being of the same order of magnitude. Reppe et al. (2025) concluded that for *Banksia* seed pods the shrinkage property gradient within the mesocarp was the result of changes in lignin content, rather than cellulose microfibril angle. Rafsanjani et al. (2014) indicated that the anisotropy seen in the swelling of the S2 layer of latewood cannot solely be explained by the microfibril angle of the cellulose fibrils. However, Lanvermann et al. (2013) showed that lignin content between earlywood and latewood was rather constant. Taking these results together, this suggest that other structural changes might influence hygroexpansion of wood.

At the meso scale, the longitudinal hygroexpansion of clear wood is much smaller than in the transverse direction. A difference in hygroexpansion is also seen between the transverse radial and tangential direction. The swelling in tangential direction can be twice to thrice as large as the radial swelling (Engelund Thybring et al., 2022). The tangential hygroexpansion is affected by a complex interaction between the expansion of earlywood, transition wood, and latewood tissue (Lanvermann et al., 2014). Isolated earlywood has larger anisotropy than isolated latewood, which can be an effect of the stiffer rays in earlywood (Engelund Thybring et al., 2022). Latewood tissue, unlike the S2 layer of latewood, swells almost isotropic (Rafsanjani et al., 2014), which

could be due to constraints initiated by the microfibril angle in the S1 and S3 layer.

The tangential swelling coefficient of earlywood tissue is larger for earlywood than for latewood, with values between 0.33 – 0.45 and 0.33 – 0.6, respectively. The radial swelling coefficients has values between 0.07 – 0.45 and 0.25 – 0.5, respectively (Lanvermann et al., 2013). Due to the difference in swelling properties between earlywood and latewood as well as the circular arrangement of the cells, the hygroexpansion in tangential direction is constrained. Shear – therefore - develops between the earlywood and latewood interface during adsorption or desorption. Despite the differences also seen in radial direction, the wood tissue is free to swell or shrink. The process in this direction is dominated by earlywood deformations, since the highest expansion is found in the dense latewood (Lanvermann et al., 2014) and related to density difference in radial direction.

On macro and structural scale, hygroexpansion is dominated by annual ring orientation, spiral grain, density differences, anisotropy, and differential shrinkage due to moisture gradients (Bengtsson, 2001; Florisson et al., 2021; Perstorper et al., 2001). Hygroexpansion contributes to high tensile stress, which makes the wood prone to cracks. Areas where the annual rings align with the outer surfaces of structural elements are prone to high tensile stress early on in the drying process. This is followed by high compression stress later on in the same process, supported by the continuous development of moisture gradients and therefore internal constraints. Another form of internal constraint arises from the differences seen in hygroexpansion properties between sapwood and heartwood, which marks the interface between these two wood types as an area also prone to tensile stress during moisture exchange (Florisson, 2021). Since a correlation exists between diffusion of moisture, density of wood and hygroexpansion coefficient of wood, a density variation also contributes to a nonuniform strain development due to hygroexpansion.

The state-of-the-art concerning hygroexpansion clearly elucidates that swelling and shrinkage properties of wood are clearly affected by structural features introduced at different hierarchical levels. Individual wood structures behave differently when isolated than when part of higher length scales. The wood seems to regulate dimensional changes at lower length scales and therewith increases the dimensional stability of the tree. This elucidates the importance of multiscale approaches with targeted research strategies.

2 – BACKGROUND

Ciesielski et al. (2020) concluded in their discussion on the advances in multiscale modelling of lignocellulosic biomass that there is (1) a lack of multiscale integration strategies that capture properties and behaviour spanning different length scales and (2) an inability of modelling approaches to effectively capture the variability and diversity of lignocellulose materials.

Multiscale simulation techniques typically fall into two categories: concurrent and hierarchical (Kwon et al., 2008). The concurrent method incorporates aspects of a phenomena at various length scales in a single simulation. Whereas, the hierarchical methods identify and quantify cause and effect relationships at lower scales and incorporate them into higher scales through information transfer.

X-ray scattering and full-field tomography enable real-time and non-destructive characterisation of wood from nano to macro material level. Small-angle X-ray scattering (SAXS) can provide the distance between microfibrils and the size of microfibril aggregates. Wide-angle X-ray scattering (WAXS), on the other hand, can provide information on the microfibril angle. These techniques are well supplemented by X-ray full-field tomography (XCT), which provides detailed images of the micro to macro material structure of wood.

Pajaanen et al. (2022) demonstrated the strong synergy between SWAXS and atomistic models in providing detailed structural insights. Whereas in Florisson et al. (2023), a similar synergy was shown between XCT and finite element modelling. The use of four-dimensional tomographic data into continuum models gives the possibility to incorporate the natural variability of material and to create realistic simulations through validation.

Linking atomistic and continuum modelling through information transfer is a rather well explored territory, but not an easy and straightforward task for an inhomogeneous and anisotropic material such as wood. In this paper, a multiscale research methodology is developed that combines atomistic and continuum modelling to get a fundamental understanding of wood hygromechanics. The modelling framework is supported by SWAXS and XCT experiments, respectively. The methodology is presented together with three case studies that represent ongoing work related to hygroexpansion.

3 – PROJECT DESCRIPTION

The developed multiscale research methodology is presented in **Figure 2**. The dark salmon coloured vertical arrow shows the hierarchical multiscale modelling strategy using information transfer. The strategy combines atomistic and continuum modelling and is able to address the first challenge by being able to span from nano scale all the way up to macro scale. The methodology can be exited after the modelling stage or continued to validate the numerical models using a combination of SWAXS and XCT. The information from SWAXS and XCT can also be used to develop the numerical models, as indicated by the light-coloured horizontal arrows. This allows the models to capture the second challenge, namely variability and diversity of material.

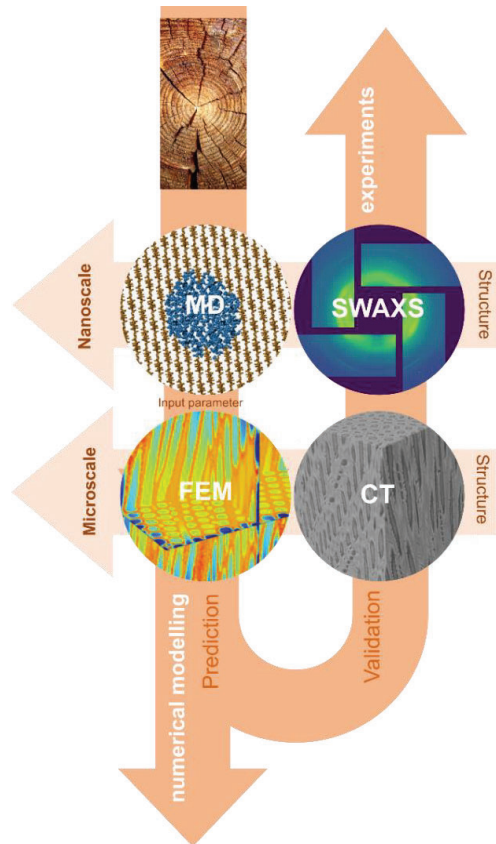


Figure 2: Developed multiscale research methodology for wood to be able to link property to structure

3.1 CASE STUDY 1: MOISTURE DIFFUSION IN NANOPORES

The wood cell wall is inherently porous due to the formation of nanopores. To capture the effect of water moving through nanopores during drying, a concentration gradient driven model is desired. An

inherent property of atomistic simulations is the rate of self-diffusion, characterised by a diffusion coefficient, which can be derived from the mean square displacement (MSD) of particles over time (Frenkel et al., 2023). Self-diffusion describes the movement of identical particles in a system where there is no concentration gradient. Diffusion on the continuum level is traditionally treated as gradient-driven, meaning it relies on a concentration gradient (or another driving force). However, self-diffusion, in its purest sense, occurs without any such gradients. Reconciling this with continuum-level analysis involves some nuances.

The first case study presents a non-equilibrium molecular dynamics simulation method to determine the concentration gradient driven diffusion coefficient of moisture in cellulose nanopores of varying shapes and sizes. This simulation system is shown in **Figure 3** and was first introduced by Frentrup et al. (2012) for other types of materials. The simulations were run in open source software LAMMPS (Plimpton, 1995; Thompson et al., 2022) and used the CHARMM forcefield (MacKerell et al., 1998) and TIP3P water model (Jorgensen et al., 1983). Cellulose-Builder (Gomes et al., 2012) and VMD (Humphrey et al., 1996) were used to prepare the system, and the charmm2lammmps subdirectory (in 't Veld et al., 2005) to convert to LAMMPS format.

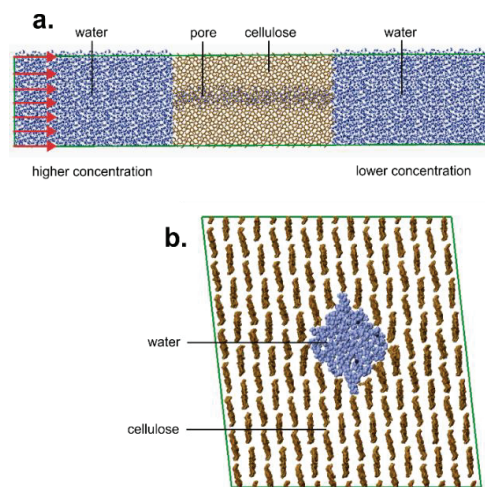


Figure 3: (a) Nanopore system and (b) cross section of the nanopore

The system consists of two opposed water basins connected through a nanopore. An external potential is applied (red arrows **Figure 3**) to a small region at the left side of the periodic simulation box using the *fix addforce* command in LAMMPS (Thompson et al., 2022). This external potential introduces a concentration gradient

between the two basins and mimics the conditions of Fick's first law of diffusion

$$q = -D\nabla c \quad 1$$

where, q is the diffusion flux through the pore, D is the diffusion coefficient in the pore direction, ∇ is the gradient tensor, and ∇c denoted the concentration gradient between the basins. This particular system was previously applied to a variety of pores and fluids (Frentrup et al., 2012). In this case study – for the first time - the method is tested in context of cellulose and water.

In **Figure 4**, a first estimation of transport diffusion coefficient is shown using different thermostatting methods. The determined diffusion coefficients provide initial values suitable in continuum modelling, bridging the gap between molecular interactions and macroscopic transport. Coming results will have to show the impact of pore morphology on the diffusivity of water and quantify the specific interactions between water and cellulose during concentration-driven transport.

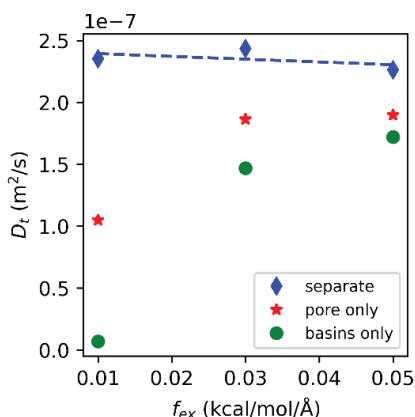


Figure 4: Transport diffusivity of the nanopore at different applied forces and for different temperature schemes at 300K.

3.2 CASE STUDY 2: ELASTICITY OF CELLULOSE

The elastic and swelling behaviours of wood are intrinsically linked. How the elastic modulus of wood at the nanoscale comes about is not yet fully understood. The elastic tensor of cellulose $I\beta$, the predominant crystalline cellulose allomorph in wood, is monoclinic rather than orthotropic as seen for wood. This is due to its intrinsic monoclinic crystal space group (Nishiyama et al., 2002). The cellulose fibrils in the wood cell wall are not uniformly distributed, but tend to cluster more in one region than the other (Fernando et al., 2023), resulting in

different sized microfibrils. The second case study aims in the long run to obtain a continuum model of wood that considers the atomistic level. As a starting point the effect of cellulose nanofibril size on associated elastic tensor is investigated. A method is proposed where this tensor is determined using atomistic simulations of a single cellulose nanofibril in water.

In this case study, the elastic tensor is determined per backbone atom by adopting Hooke's law

$$\sigma = E\varepsilon \quad 2$$

Stress and strain are fundamentally continuum quantities, and their computation from microscopic interactions in an atomistic simulation can be cumbersome. The theoretical frameworks do not always match and require insightful approaches to overcome. The definition of atomic virial stress is used to determine the three-dimensional symmetric per atom stress tensor. The simulations were made in LAMMPS using forcefields CHARMM for cellulose and TIP3P for water. To be able to compute the stress tensor for the cellulose system, the `compute stress/atom` command in LAMMPS (Thompson et al., 2022) was used

$$S_{ab} = -mv_a v_b - W_{ab} \quad 3$$

where, the first term is a kinetic energy contribution for the current atom and indices a and b refer to the considered atom and neighbouring atoms, respectively. The second term is the virial contribution due to intra and intermolecular interactions. For a full description, the reader is referred to the online manual of LAMMPS.

The computation of strain using atomic positions at discrete time intervals requires either interpolation of a continuous displacement field or a discretisation of the gradient operator. In this study, the latter is chosen as proposed in Gullett et al. (2008), and the strain is computed using Green-Lagrange theorem

$$\begin{aligned} E &= \frac{1}{2}(\hat{\mathbf{F}}^T \hat{\mathbf{F}} - \mathbf{I}) \\ \hat{\mathbf{F}} \mathbf{D} &= \mathbf{A} \\ \mathbf{D} &= \sum_n \Delta \mathbf{X}^{mn} \Delta \mathbf{X}^{mnT} w_n \\ \mathbf{A} &= \sum_n \Delta \mathbf{x}^{mn} \Delta \mathbf{x}^{mnT} w_n \end{aligned} \quad 4$$

where $\hat{\mathbf{F}}$ is the discrete deformation gradient, $\Delta \mathbf{X}^{mn}$ is the relative position of neighbouring atom n to considered

atom m in the undeformed configuration, Δx^{mn} represent the same, but in the deformed configuration, and w_n is a weight factor. \mathbf{E} is the Green-Lagrange strain tensor, where \mathbf{I} represents an identity matrix. This interpretation of strain is in respect to the reference coordinates. The derivation of this form of the strain tensor can be found in Gullett et al. (2008), together with a more detailed description of the weight factor.

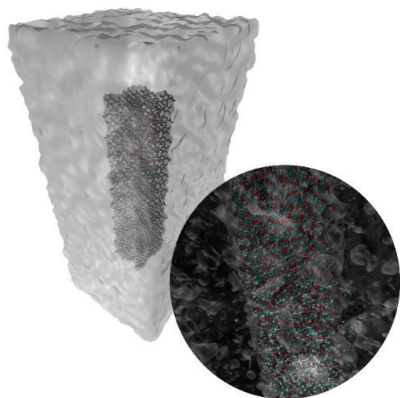


Figure 5: Visualisation of the computational system that contains a four-by-four chain cellulose system in water

The proposed method to compute the deformation gradient, strain tensor and stress tensor makes the approach useful for evaluation of continuum models and mechanical property relationships. Different cellulose structures are investigated to observe a possible size effect on the elastic tensor. For simplicity, the cellulose nanofibril is modelled as rectangular cross sections (four-by-four, six-by-six, twelve-by-twelve and full simulation box). In **Figure 5**, the cellulose system of a four-times-four microfibril in water is shown. A load is applied using the *fix smd cfor* command in LAMMPS (Thompson et al., 2022) in all relevant configurations to fill a three-dimensional elastic tensor. This applies a constant force between the centre-of-mass of two atom groups.

In **Figure 6**, the computed Green Lagrange strain for a cellulose backbone loaded with a $8000 \text{ kJ mol}^{-1} \text{ nm}^{-1}$ constant force. Coming results will have to confirm whether the elastic tensor is monoclinic and size dependent. A representative volume element is identified, and the tensorial distance is used to identify non-apparent symmetry classes.

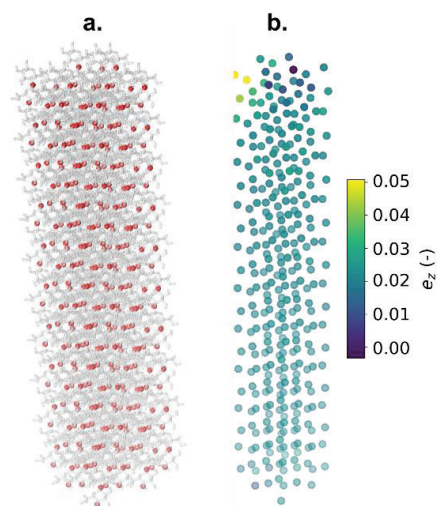


Figure 6: Green Lagrange strain computed for cellulose backbone applying a constant force of $8000 \text{ kJ mol}^{-1} \text{ nm}^{-1}$ along the lengthwise direction.

3.3 CASE STUDY 3: HYGROEXPANSION OF BRANCH WOOD

The hygroexpansion of branch wood is highly under investigated. The cross section of Norway spruce branches clearly consists of opposite wood at the upper side of the branch and compression wood at the lower side. To better understand the swelling differences seen between these two wood types, atomistic swelling models of lignin were used to obtain swelling properties of this chemical component and continuum models of the S2 cell wall layer were used to investigate the effect of these properties on micro material level.

Two systems of 1000 lignin tetramers under varying moisture content were investigated using molecular dynamics. The first system is opposite wood lignin represented by an all-guaiacyl tetramer, with four β -O-4' linked coniferyl units. The second system is compression wood lignin for which one of the coniferyl units is exchanged by a 4-hydroxyphenyl unit. The simulations were performed in GROMACS using the CHARMM force field for lignin and the TIP3P model for water. The interaction between water and lignin and the swelling of the entire box were observed for 20 different levels of moisture content ranging between 0.1 and 0.26 (-). A detailed description of the system setup can be found in (Hartwig-Nair et al., 2025).

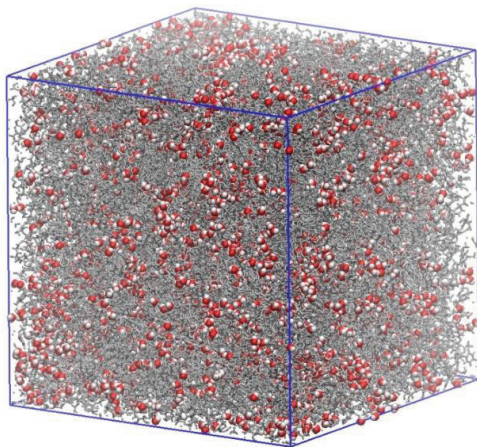


Figure 7: A representation of the simulation system for atomistic modelling. The grey molecules represent lignin and the red and white molecules represent water (Hartwig-Nair et al., 2025)

The hygroexpansion of the S2 layer was investigated using finite element modelling and generalised plane strain

$$\begin{pmatrix} \varepsilon_{xx} \\ \varepsilon_{yy} \\ \varepsilon_{zz} \\ \gamma_{xy} \end{pmatrix} = \begin{pmatrix} 1/E_x & -\nu_{yx}/E_y & -\nu_{zx}/E_z & 0 \\ -\nu_{xy}/E_x & 1/E_y & -\nu_{zy}/E_z & 0 \\ -\nu_{xz}/E_x & -\nu_{yz}/E_y & 1/E_z & 0 \\ 0 & 0 & 0 & 1/2G_{xy} \end{pmatrix} \begin{pmatrix} \sigma_{xx} \\ \sigma_{yy} \\ \sigma_{zz} \\ \sigma_{xy} \end{pmatrix} + \begin{pmatrix} \beta_x \\ \beta_y \\ \beta_z \\ 0 \end{pmatrix} \Delta c \quad 5$$

where, ε and γ represent strain, E is the elastic modulus, G is the shear modulus, ν is the Poisson's ratio, σ is stress, β is the swelling coefficient, and c indicates concentration. A full overview of theory and material properties used for the simulation of opposite and compression wood can be found in (Hartwig-Nair, 2024).

The representative unit cell of the S2 cell wall layer visualised in **Figure 8** was made in COMSOL® Multiphysics® v. 6.1 (COMSOL Multiphysics® v. 6.1 2025). The unit cell is composed of nine cellulose microfibrils with square cross-sections of 3.5 times 3.5 nm². The distance between the microfibril is 0.35 nm. Hemicellulose is wrapped around and placed in between the microfibrils. Lignin is then subsequently wrapped around the hemicelluloses. The ratios of these chemical components defining the difference between opposite and compression wood are based on literature and a full summary is given in Hartwig-Nair (2024). Opposite

wood has more cellulose, where compression wood has more hemicellulose and lignin. Periodic boundary conditions were applied on the boundaries of the unit cell to allow for free expansion. A uniform cubic mesh of 0.1 nm was chosen.

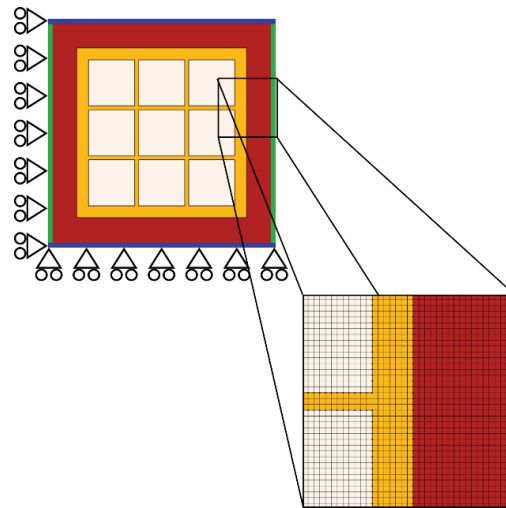


Figure 8: Geometric model of a fraction of the S2 cell wall layer used for finite element modelling including boundary conditions and mesh. Red is lignin, yellow is hemicellulose and white is cellulose.

The finite element model coupled changes in molecular structure of branch wood to swelling behaviour at the microstructural scale through information transfer.

The study confirmed that lignin content and lignin swelling influences the swelling behaviour of the S2 layer (Hartwig-Nair, 2024). These properties, together with the difference seen in microfibril angle between opposite and compression wood, result in a larger longitudinal swelling coefficient (z' in **Table 1**) for compression wood than for opposite wood and a larger transverse swelling coefficient (y' in **Table 1**) for opposite wood than for compression wood (Hartwig-Nair, 2024), as is expected for these wood types.

The results also showed that if we consider the swelling coefficient of lignin, lignin content and microfibril angle in the finite element model and measure the swelling coefficient of the S2 layer, compression wood swells about twice as much (see **Table 1**). This does not explain the measure of swelling difference seen between opposite and compression wood at tissue level, and suggests that other phenomena are at hand that explain this difference.

Table 1: Swelling coefficient, β , obtained for opposite (OW) and compression wood (CW) with the model of the S2 layer compared to the swelling coefficients obtained for OW and CW lignin, β_L , using molecular dynamics, including the lignin content (LC) and microfibril angle (MFA)

dir	β		β_L		LC		MFA	
	CW	OW	CW	OW	CW	OW	CW	OW
z'	0.147	0.094	0.350	0.353	42%	34%	53°	41°
y'	0.086	0.123						

6 – CONCLUSION

A framework is presented to facilitate a multiscale interpretation of the hygroexpansion of wood both on nano and micro structural level using numerical and non-destructive X-ray techniques. This approach should tackle the lack of multiscale integration strategies available for wood and an inability of modelling approaches to capture the variability of material. The numerical part of the framework is tested on several case studies. The case studies clearly show that information transfer between the nano and micro scale is not a swift process, but often requires accommodation of simulation models and results. However, the case studies also showed that with the right approach the research methodology can provide detailed material properties for continuum modelling and a fundamental view on different phenomena associated with hygroexpansion of wood.

7 – ACKNOWLEDGEMENT

This work was supported by the Swedish Research Council (Vetenskapsrådet) under grant number 2023-04705 and the National Academic Infrastructure for Supercomputing in Sweden (NAISS) for the provided computational resources under projects NAISS 2025/22-356, 2025/5-83 and 2024/22-1669.

8 – REFERENCES

- COMSOL Multiphysics® v. 6.1 (2025). www.comsol.com. . COMSOL AB.
- Bengtsson, C. (2001). Variation of moisture induced movements in Norway spruce (*Picea abies*). *Annals of Forest Science*, 58, 569-581.
- Chen, P., Wohlert, J., Berglund, L., & Furó, I. (2022). Water as an intrinsic structural element in cellulose fibril aggregates. *The Journal of Physical Chemistry Letters*, 13, 5424-5430.
- Ciesielski, P. N., Brennan Pecha, M., Lattanzi, A. M., Vivek Bharadwaj, S., Crowley, M. F., Bu, L., Vermaas, J. V., Xerxes Steirer, K., & M.F., C. (2020). Advances in multiscale modeling of lignocellulosic biomass. *ACS Sustainable Chemistry and Engineering*, 8, 3512-3531.
- Engelund Thybring, E., Fredriksson, M., Zelinka, S. L., & Glass, S. V. (2022). Water in wood: A review of current understanding and knowledge gaps. *Forests*, 13, 2051.
- Fernando, D., Kowalczyk, M., Guindos, P., Auer, M., & Daniel, G. (2023). Electron tomography unravels new insights into fiber cell wall nanostructure; exploring 3D macromolecular biopolymeric nano-architecture of spruce fiber secondary walls. *Scientific Reports*, 13(2350).
- Florisson, S. (2021). *Moisture-induced stress and distortion of wood: A numerical and experimental study of wood's drying and long-term behaviour* [Doctoral thesis, Linnaeus University]. Växjö, Sweden.
- Florisson, S., & Gamstedt, E. K. (2023). An overview of lab-based micro computed tomography aided finite element modelling of wood and its current bottlenecks. *Holzforschung*, 77(11-12), 793-815.
- Florisson, S., Vessby, J., & Ormarsson, S. (2021). A three-dimensional numerical analysis of moisture flow in wood and of the wood's hygro-mechanical and visco-elastic behaviour. *Wood Science and Technology*.
- Frenkel, D., & Smit, B. (2023). *Understanding molecular simulation: From algorithms to applications*. Academic Press.
- Frentrup, H., Avendaño, C., Horsch, M., Salih, A., & Müller, E. A. (2012). Transport diffusivities of fluids in nanopores by non-equilibrium molecular dynamics simulation. *Molecular Simulation*, 38(7), 540-553.
- Gomes, T. C. F., & Skaf, M. S. (2012). Cellulose-Builder: A toolkit for building crystalline structures of cellulose. *Journal of Computational Chemistry*, 33, 1338-1346.
- Gullett, P. M., Horstemeyer, M. F., Baskes, M. I., & Fang, H. (2008). A deformation gradient tensor and strain tensors for atomistic simulations. *IOP Publishing*, 16, 015001.
- Hartwig-Nair, M. (2024). *Structure and hygroelastic properties of conifer branch wood: A multiscale approach*. [Doctoral thesis, Uppsala University]. Uppsala, Sweden.
- Hartwig-Nair, M., Florisson, S., Wohlert, M., & Gamstedt, E. K. (2024). Characterisation of hygroelastic properties of compression and opposite wood found in branches of Norway spruce. *Wood Science and Technology*, 58, 887-906.
- Hartwig-Nair, M., Nasedkin, A., Hackenstrass, K., De Santis, E., Florisson, S., & Wohlert, M. (2025). Lignin hygroexpansion in compression and opposite wood - a molecular dynamics study. *Wood Science and Technology*, 59(21).
- Humphrey, W., Dalke, A., & Schulten, K. (1996). VMD: Visual Molecular Dynamics. *Journal of Molecular Graphics*, 14, 33-38.

- in 't Veld, P. J., & Crozier, P. (2005). *ch2lmps subdirectory*. In Github. <https://github.com/lammps/lammps/blob/develop/tools/ch2lmp/>
- Jakes, J. E., Hunt, C. G., Zelinka, S. L., Ciesielski, P. N., & Plaza, N. Z. (2019). Effects of moisture on diffusion in unmodified wood cell walls: A phenomenological polymer science approach. *Forests*, *10*(1084).
- Jorgensen, W. L., Chandrasekhar, J., Madura, J. D., Impey, R. W., & Klein, M. L. (1983). Comparison of simple potential functions for simulating liquid water. *The Journal of Chemical Physics*, *79*(2), 926-935.
- Kwon, Y. W., Allen, D. H., & Talreja, R. (2008). *Multiscale modeling and simulation of composite materials and structures*. Springer.
- Lanvermann, C., Evans, R., Schmitt, U., Hering, S., & Niemz, P. (2013). Distribution of structure and lignin within growth rings of Norway spruce. *Wood Science and Technology*, *47*, 627-641.
- Lanvermann, C., Wittel, F. K., & Niemz, P. (2014). Full-field moisture induced deformation in Norway spruce: intra-ring variation of transverse swelling. *European Journal of Wood and Wood Products*, *72*, 43-52.
- Lim, J. H. (2024). *Order and disorder in cellulose microfibrils* [Doctoral thesis, Université Grenoble Alpes]. Grenoble, France.
- MacKerell, A. D., Bashford, D., Bellott, M., Dunbrack, R. L., Evanseck, J. D., Field, M. J., Fischer, S., Gao, J., Guo, H., Ha, S., Joseph-McCarthy, D., Kuchnir, L., Kuczera, K., Lau, F. T. K., Mattos, C., Michnick, S., Ngo, T., Nguyen, D. T., Prodhom, B., Reiher III, W. E., Roux, B., Schlenkrich, M., Smith, J. C., Stote, R., Straub, J., Watanabe, M., Wiórkiewicz-Kuczera, J., Yin, D., & Karplus, M. (1998). All-atom empirical potential for molecular modeling and dynamics studies of proteins. *Journal of Physical Chemistry B*, *102*(18), 3586-3616.
- Nishiyama, Y. (2023). Thermodynamics of the swelling work of wood and non-ionic polysaccharides: A revisit. *Carbohydrate Polymers* *320*, 121227.
- Nishiyama, Y., Langan, P., & Chanzy, H. (2002). Crystal structure and hydrogen-bonding system in cellulose I β from synchrotron X-ray and neutron fiber diffraction. *Journal of the American Chemical Society*, *124*(31).
- Pajaanen, A., Zitting, A., Rautkari, L., Ketoja, J. A., & Penttilä, P. A. (2022). Nanoscale mechanism of moisture-induced swelling in wood microfibril bundles. *Nano Letters*, *22*, 5143-5150.
- Perstorper, M., Johansson, M., Klinger, R., & Johansson, G. (2001). Distortion of Norway spruce timber: Part I Variation of relevant wood properties. *Holz als Roh- und Werkstoff*, *59*, 94-103.
- Plimpton, S. (1995). Fast parallel algorithms for short-range molecular dynamics. *Journal of Computational Physics*, *117*, 1-19.
- Rafsanjani, A., Stiefel, M., Jefimovs, K., Mokso, R., Derome, D., & Carmeliet, J. (2014). Hygroscopic swelling and shrinkage of latewood cell wall micropillars reveal ultrastructural anisotropy. *Journal of The Royal Society Interface*, *11*, 20140126.
- Reppe, F., Guiducci, L., Elbaum, R., Werner, P., Dunlop, J. W. C., Merritt, D. J., Fratzl, P., & Eder, M. (2025). Material composition gradient controls the autonomous opening of Banksia seed pods in fire-prone habitats. *Advanced Functional Materials*, *2418592*.
- Thompson, A. P., Aktulga, H. M., Berger, R., Bolintineanu, D. S., Brown, W. M., Crozier, P. S., in 't Veld P. J., Kohlmeyer, A., Moore, S. G., Nguyen, T. D., Shan, R., Stevens, M. J., Tranchida, J., Trott, C., & Plimpton, S. J. (2022). LAMMPS - a flexible simulation tool for particle-based materials modeling at the atomic, meso, and continuum scales. *Computer Physics Communications*, *271*, 10817.
- Zhang, C., Chen, M., Keten, S., Coasne, B., Derome, D., & Carmeliet, J. (2021). Hygromechanical mechanisms of wood cell wall revealed by molecular modeling and mixture rule analysis. *Science Advances Research Article*, *7*, eabi8919.